Pressure dependence of laminar-turbulent transition in gases

L. D. Hinkle[a)]
Falmouth Public Schools, Falmouth, Massachusetts 02536

A. Muriel
Department of Physics, Hong Kong University of Science and Technology, Kowloon, Hong Kong

S. A. Novopashin
Institute of Thermophysics, 630090 Novosibirsk, Russia

The transition between the laminar and turbulent flow regimes is traditionally addressed using the continuum formulation of the Navier-Stokes equations and dimensionless parameters such as the Reynolds number. However, a detailed understanding of the transition mechanisms has remained elusive. Theoretical approaches based on molecular and quantum mechanical models have been proposed but have yet to be thoroughly tested experimentally. In an effort to test a quantum-based model, specific apparatus and experiments have been designed to evaluate particular features of the laminar-turbulent transition. Hysteresis plots of flow versus differential pressure are used to examine the flow transition that occurs inside a tube with a divergent entrance. The hysteresis plots generated in these tests show several notable features and quantitative trends. The primary focus of this article is on the observed dependence of the laminar-turbulent transition behavior on the absolute pressure. Whereas the continuum-based model does not predict a pressure dependence of the laminar-turbulent transition, a molecular-based model indicates a pressure effect on the transition to turbulent flow. © 2006 American Vacuum Society. [DOI: 10.1116/1.2197506]

I. INTRODUCTION

The parameters that traditionally characterize the laminar and turbulent regimes of gas flow in channels are the macroscopic quantities—channel dimension, density, mean velocity, and viscosity. Generated from these parameters, the Reynolds number (R_e) has been used empirically to reasonably predict the regime of flow for gases in viscous flow.[1] However, R_e is at best only a guideline for the behavior. Furthermore, a macroscopic description of the laminar-turbulent transition mechanism based on the Navier-Stokes equations (NSEs) has not been successfully developed despite significant incentive and effort.[2–4]

One alternative to understanding and describing the laminar-turbulent transition assumes a molecular-based or quantum-based mechanism. While several approaches in this vein have been attempted,[5–14] this remains controversial in the field of fluid mechanics as none has yet been sufficiently verified experimentally.[15–18] The development of experimental methods to uncover observable phenomena related to the transition is essential in the pursuit and verification of hypotheses for the underlying mechanisms for the transition. To observe characteristic and distinguishing behavior one is motivated to find circumstances where the scale invariance of the NSE-based continuum model is violated. While several possible methods of varying parameters can be devised to test for scale invariance, the pressure of the gas is the chosen parameter varied for the work reported here. The interesting pressure range for this study was revealed to be in the sub-atmospheric viscous flow regime—and well away from the sonic flow and molecular flow regimes.

II. APPARATUS

The data presented here have been obtained using two different experimental setups, one in the United States and the other in Russia. Although the two apparatus' construction, operation, data time scales, and spatial scales are quite different, they each demonstrate similar phenomena regarding the laminar/turbulent transition behavior.

The US experimental setup was based on a previously reported apparatus.[19] However, several modifications had been made to (1) control the downstream pressure and (2) measure the differential pressure across the test artifact—a divergent glass pipette with an inner diameter of 0.8 mm at its entrance, gradually expanding to 2.5 mm over an axial length of 2 cm—where the transition occurs. Figure 1 shows a schematic overview of the apparatus. The operation of the apparatus consists of controlling the inlet flow and measuring the artifact flow, absolute pressure, and differential pressure. The entry of gas is regulated by a mass flow controller (MKS Type 1179A 2 slm full scale) which is connected to a 0.15 liter upstream chamber. The test artifact serves as the upstream chamber outlet, with the narrow end of the artifact positioned approximately 2 cm inside of and sealed to the chamber wall. The wide end is connected via a *T* fitting to a high-speed micromachined flowmeter (TSI Model 4121) and a micromachined differential pressure sensor (Honeywell Microswitch 142PC01D). The differential pressure sensor is arranged such that the primary port is connected to the up-

---
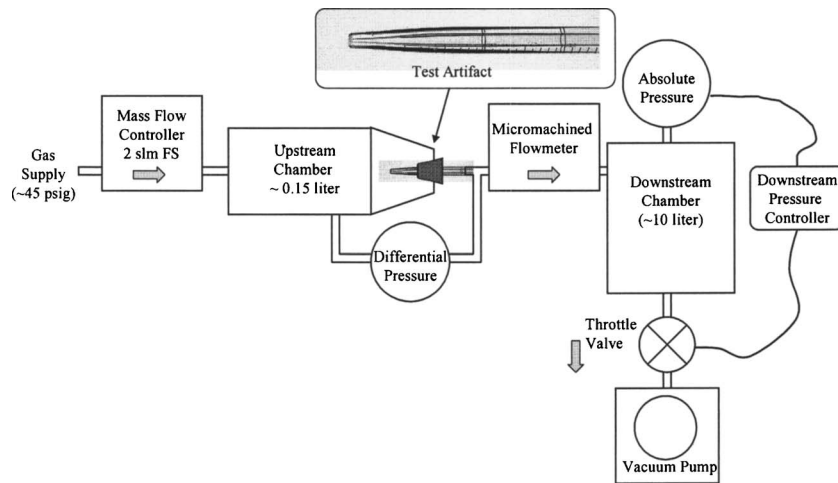
a)Electronic mail: luketech@earthlink.net

FIG. 1. Schematic diagram of the US apparatus.

stream chamber while the reference is connected to the downstream side of the artifact. The micromachined flowmeter outlet is connected to a relatively large (~10 liter) downstream chamber which is pressure controlled via a capacitance manometer (MKS Type 122 1000 Torr) and throttle valve (MKS Type 253). The MKS Controller Type 252 adjusts the throttle valve to control the downstream chamber pressures over the range from 200 to 1000 Torr. Prior to testing, the flow controller calibration was verified directly with a primary flow standard (MKS Califlow® A200) for both nitrogen and argon gases. In turn, the TSI flowmeter calibration was directly compared with the flow controller *in situ* with each of the test gases over the experimental pressure range by replacing the test artifact in the apparatus with a large-bore tube. These calibration data were subsequently used to generate a second-order polynomial fit which was then applied as a correction to the TSI flowmeter readings in units of standard liters per minute (slm).

The apparatus constructed in Russia is also a modification of one that had been previously reported.[15,20,21] The experimental setup is shown in Fig. 2. The chamber (approximately 10 liters) can be pumped to rough vacuum to initialize operation. To provide a short characteristic time of heat exchange between the gas and chamber, the chamber was filled by a rolled sheet of stainless steel mesh. This provides effectively isothermal conditions during gas inflow and outflow. The gas supply system includes a high pressure reservoir, pressure reducer, and control valve. The pressure before the control valve is typically set to 5 atm. This ensures critical flow conditions at the inlet restriction resulting in a flow rate that is independent of the pressure in the chamber. The test artifact exhausts to ambient pressure through an outlet valve. The artifact used for the data presented here is similar, but dimensionally different from that used in the US apparatus. It is a divergent glass tube with a 0.75 mm inner diameter at its inlet, gradually increasing to a 2.5 mm inner diameter over an axial length of 2.5 cm and continuing for 27 cm to its outlet. A differential pressure sensor (ИКДф-0.1) is used to measure the pressure inside the tank, with reference to the ambient pressure. Thus, the pressure drop across the artifact

is effectively measured over the range of 0.01–50 Torr with a maximum measurement sample rate of 1 kHz and peak-to-peak noise of 0.04 Torr. Inflow rate is independently measured for each setting of the control valve and supply pressure by closing the outlet valve and monitoring the differential pressure rise rate. Similarly, differential pressure data are used to calculate the test artifact flow rate and pressure difference versus time at various chamber inflow rates. Calculations include the second virial coefficient in the equation of state for each gas which applies a flow correction (relative to the ideal gas case) of less than 2% for the gases reported here. Temperature was controlled with the accuracy of 0.5 °C. All series of experiments have been carried out within the temperature range of 20–25 °C. Test gases used in this apparatus have been nitrogen, argon, sulfur hexafluoride, and carbon dioxide.
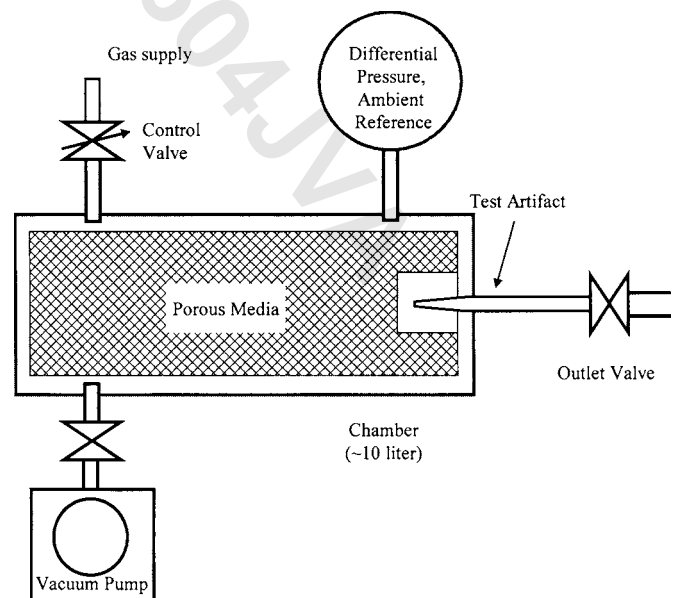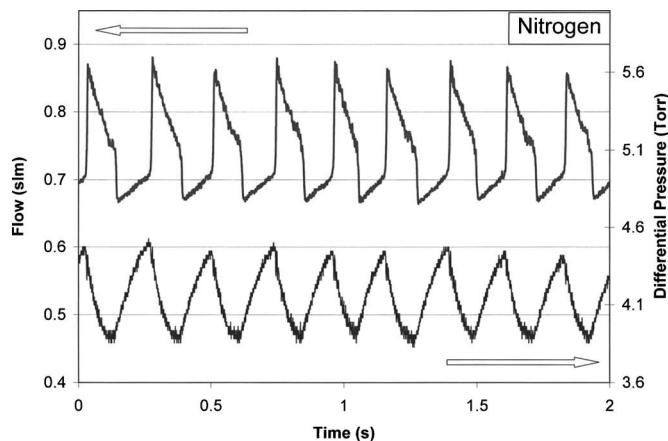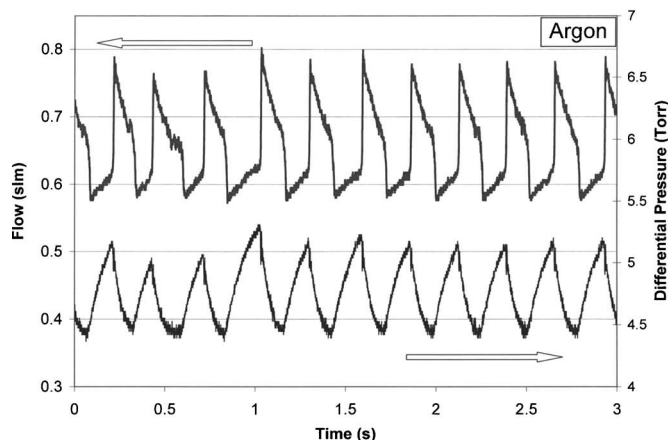

FIG. 2. Schematic diagram of the Russian apparatus.

J. Vac. Sci. Technol. A, Vol. 24, No. 4, Jul/Aug 2006

PROOF COPY 068604JVA

(a)

(b)

FIG. 3. (a) Behavior of flow vacillation in US apparatus for nitrogen with an outlet pressure of 765 Torr. (b) Behavior of flow vacillation in US apparatus for argon with an outlet pressure of 765 Torr.

III. RESULTS AND DISCUSSION

Both apparatuses demonstrate a condition where the flow in the artifact cannot exist in steady state—too high for laminar and too low for turbulent flow. Also, both apparatuses
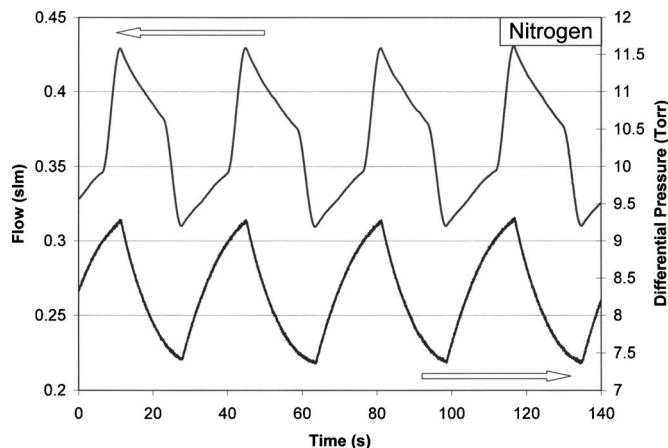

FIG. 4. Behavior of flow vacillation in Russian apparatus for nitrogen.

exhibit spontaneous, bistable behavior characterized by artifact flow vacillation when the inlet flow is set at any point between the artifact's maximum laminar flow and minimum turbulent flow.

A. Operation

First, it is important to understand the mechanism for the vacillation in this type of system and to compare the behavior to what might be called laminar-turbulent intermittency.[22–26] The self-regulated vacillations observed here are perhaps controlled versions of the long-observed spontaneous turbulent phenomena variously labeled as "flashes," "puffs," or "turbulent spots"—none of which are precisely defined. Quoting a passage from a text by Reda Mankbadi, "currently it is not clear what processes within the spot are characteristic of fully developed turbulence and what processes are unique to the spot."[27] The bistable behavior in this system results from the fact that there is higher conductance in turbulent flow than in laminar flow for this type of divergent pipe artifact. With this criterion, a vacillation cycle can be understood by beginning with the artifact flow in the laminar (lower flow) state. Since the inlet flow is controlled at a higher rate, the pressure increases in the chamber. This causes the artifact flow to increase until it transitions to turbulent flow. Once in turbulent flow, the artifact flow is higher than the inlet flow, so the chamber pressure decreases, which in turn causes the artifact flow to decrease to the point where it transitions to laminar flow again. For a given gas type the frequency of these vacillation cycles depends primarily on the chamber volume and the difference between the highest laminar flow rate and lowest turbulent flow rate. Each of the systems outlined above demonstrates this behavior, despite the significant differences in operation, scale, and instrumentation approach.

B. Results

Figure 3(a) shows data for the US system using nitrogen when the outlet pressure is controlled to approximately 1 atm (765 Torr). The apparent noise on the flow signal is actually, in part, flow oscillation which occurs near the transition point, as has been reported earlier.[19] Figure 3(b) shows the equivalent data when using argon. Note that for this system the time scale for a laminar-turbulent-laminar transition cycle is on the order of 0.25 s. Figure 4 shows the results of a similar test using nitrogen with the Russian system. Here, the qualitative behavior is the same, but because of the larger chamber volume, the time scale is significantly longer (at nearly 40 s) than that of the US system. Also, the data do not show the same level of "noise" due to the implicit time averaging of the measurement and instrumentation approach. What is observed in both systems is not intermittency or instability in the flow regime at the artifact, but rather the systematic vacillation cycle as described above.

The behavior of these data at the laminar-turbulent transition points is the focus of this investigation. A particularly useful presentation of these data is a flow versus differential
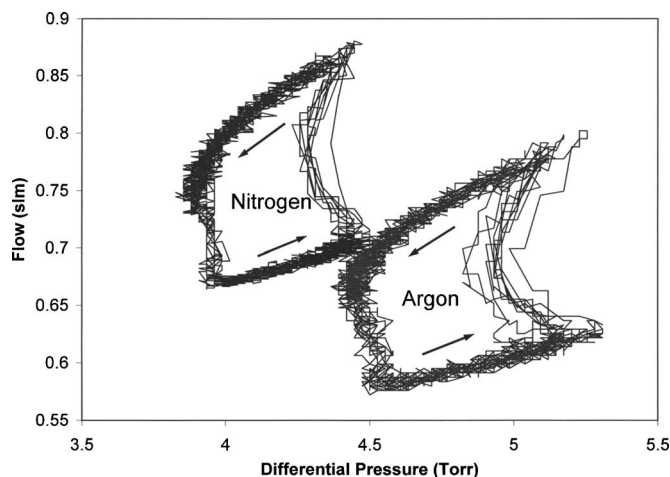
FIG. 5. Flow vs differential pressure hysteresis plots for nitrogen and argon with an outlet pressure of 765 Torr.

pressure plot. The result is a kind of hysteresis loop as shown in Fig. 5 for the data already displayed in Fig. 3. The trajectory is counterclockwise with the upper side being in the turbulent regime, the lower in the laminar regime, and the transitions occurring where the loop path becomes vertical.

The corners of the loop, points just before and after the transitions, show an interesting gas type and absolute pressure behavior. Studying the effects of gas type was the design target for the Russian system, since the flow and pressure measurements are independent of gas type, but there is no provision to control the absolute pressure at the flow artifact. The effect of absolute pressure was the area of interest studied with the US system and will be the focus for the rest of the results reported here.

Plots of the hysteresis cycles for various downstream absolute pressures are shown as Figs. 6(a) and 6(b) for nitrogen and argon, respectively. Several features for both gas types are worth noting:

(1) The hysteresis loop area decreases as the absolute pressure decreases until the effect collapses entirely at pressures between 400 and 500 Torr for the system shown in Fig. 1.
(2) The minimum laminar flow remains constant (within 3%) over the tested pressure range, while the maximum turbulent flow changes by over 30%.

In some ways, these results are in agreement with the continuum model—the laminar flow values at the transition points are relatively independent of the pressure and correspond to a R_e of approximately 2000 for each gas. In other ways, these results challenge a continuum-based model—the pressure dependence of the turbulent flow at the transitions, the collapse of the transition behavior. These phenomena occur at pressures and flow well within the usual viscous, incompressible flow boundaries. In fact, the collapse occurs under the conditions of a Knudsen number of ~ 0.0001 and a Mach number of ~ 0.1 at the artifact inlet.

To illustrate the time-base behavior of the hysteresis collapse, Fig. 7 shows flow versus time for nitrogen at several
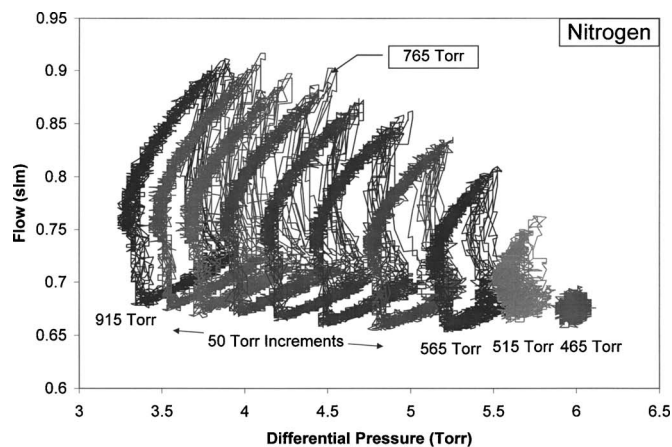
(a)
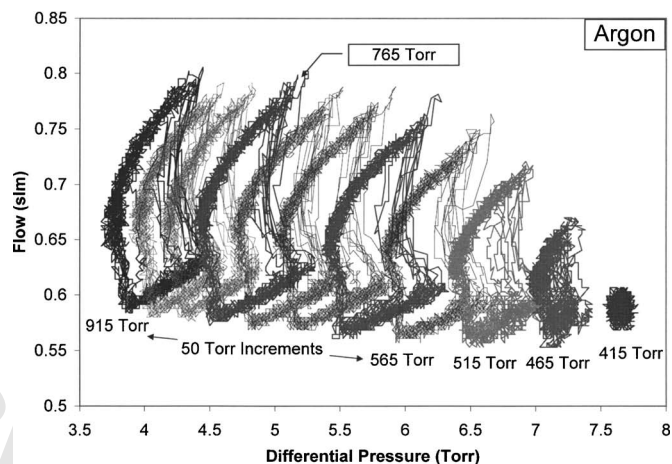
(b)

FIG. 6. (a) Hysteresis loop collapse for nitrogen. (b) Hysteresis loop collapse for argon.

absolute pressures approaching the collapse. Noticeable in the hysteresis loops and in this plot is that the "forbidden flow" gap (between the minimum turbulent and maximum laminar flows) becomes progressively smaller as the absolute pressure is decreased. As the absolute pressure approaches the condition of collapse, the gap closes and characterization as laminar or turbulent based on their distinctive conductance difference is lost.

The data presented in Figs. 3 and 5–7 were all collected using a single flow artifact. However, the same tests have been performed with a mechanically similar pipette that demonstrates the laminar-turbulent transition at higher flow (nitrogen at 0.95 slm and argon at 0.85 slm), as shown in Fig. 8. A slightly larger inner diameter and/or different entrance profile may easily explain the higher transition flow. More interesting is the hysteresis collapse which occurred at a lower pressure—between 250 and 300 Torr for both gases.

C. Mechanism for the transition collapse

One concern regarding these data and, in particular, the mechanism for the transition collapse is the role of the upstream chamber volume. Its pressure response to the dy-
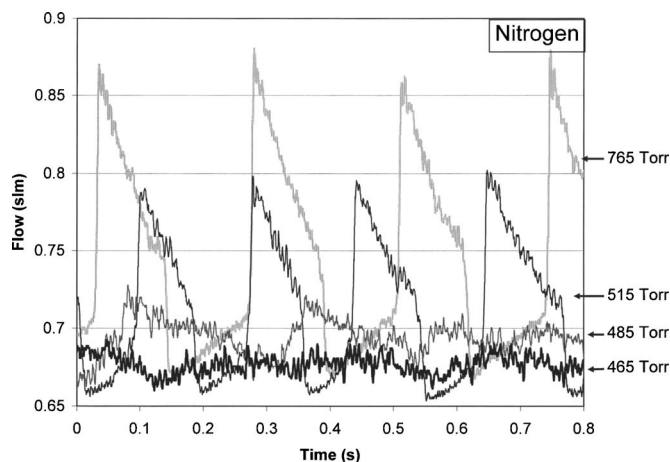
FIG. 7. Time-base flow as the pressure approaches the collapse condition for nitrogen.

namic difference in the flows (inlet and outlet) is a factor in determining the cycle frequency of the hysteresis loop. One may therefore wonder, if the combined volume and absolute pressure become too small, could this result in an inability for the flow to vacillate between distinctly laminar and turbulent? System dynamic analysis based on the first-order mass flow, pressure, and volume differential equation reveals that this scenario is not the case and cannot be responsible for the transition collapse. This has been experimentally supported by tests where the flow is gradually ramped through the transition point at various absolute pressures. The same diminishing transition phenomena have been observed as a function of decreasing absolute pressure.

The mechanism for the transition collapse may be related to the gas compressibility. If one speculates that the trigger for the transition is highly sensitive to molecule-molecule interactions, then the compressibility may be a valid metric to express this effect. So while the usual guideline for the assumption of incompressibility ($M < 0.3$) is met, perhaps the laminar-turbulent transition behavior is affected by very subtle changes in compressibility—even for Mach numbers below 0.1. This being a matter of chaotic, fluctuating behav-
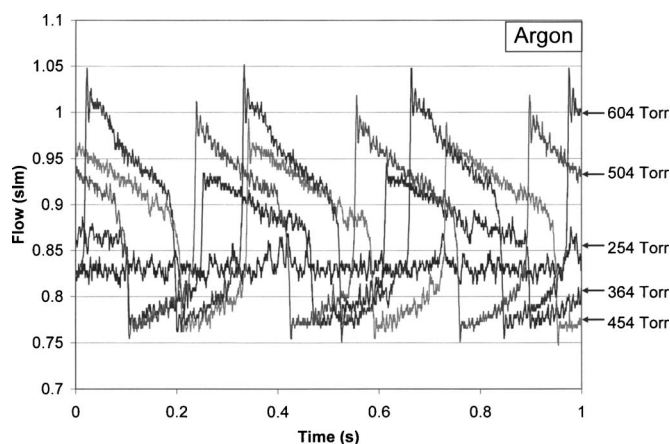
ior, that kind of sensitivity is not out of the question. Examining the results for the two artifacts, one had a higher mass flow but a lower absolute pressure at the transition collapse. When considering the inner diameter, d, and pressure relation to the Reynolds number and Mach number, it is shown that

$$M \sim R_e/(Pd),$$

so it is expected that for a given critical R_e, the larger diameter artifact will require a lower absolute pressure for the same Mach number. Thus, the pressure results are at least qualitatively consistent with an effect characterized by compressibility. While it is premature to speculate further, it is worth noting that a critical R_e dependence on the second virial coefficient has been previously reported.[20,21] Hence, this reinforces the thought that molecule-molecular interactions are responsible for the collapse of the laminar-turbulent transition.

IV. CONCLUSION

Two separate apparatuses have been developed to study the detailed pressure and flow behavior of the laminar-turbulent transition in a diverging tube artifact. A series of tests investigating the laminar-turbulent transition has shown interesting behavior as a function of absolute pressure with nitrogen and argon. A particularly useful plot of the flow versus differential pressure demonstrates a hysteresis of the transition that appears to collapse at sufficiently low absolute pressure. While the conditions at the collapse are still within the usual viscous, incompressible region of parameter space, the behavior indicates a possible molecular interaction effect characterized by the Mach number. Further investigation into the laminar-turbulent transition in this area of the parameter space is warranted. This and future experimental study may guide and/or verify theoretical approaches to understanding the molecular-level mechanism for the laminar-turbulent transition in gases.

FIG. 8. Transition collapse for second artifact using argon.

[1]U. Frisch, *Turbulence: The Legacy of A.N. Kolmogorov* (■, Cambridge, 1995).
[2]Clay Institute of Mathematics, http://www.claymath.org/millennium/ Navier-Stokes_Equations/
[3]C. M. White and K. A. Sreenivasan, Phys. Lett. A **238**, 323 (1998).
[4]C. J. Swanson, B. Julian, G. G. Ihas, and R. J. Donnely, J. Fluid Mech. **461**, 51 (2002).
[5]H. Chen, ■. Kandasamy, S. Orszag, R. Shock, S. Succi, and V. Yakhot, Science **301**, 633 (2003).
[6]A. Muriel and M. Dresden, Physica D **81**, 221 (1995).
[7]A. Muriel and M. Dresden, Physica D **94**, 103 (1996).
[8]A. Muriel and M. Dresden, Physica D **101**, 299 (1997).
[9]A. Muriel, P. Esguerra, L. Jirkovsky, and M. Dresden, Physica D **119**, 381 (1998).
[10]A. Muriel, Physica D **124**, 225 (1998).
[11]A. Muriel, Physica A **305**, 379 (2002).

[12] A. Muriel, Physica A **322**, 139 (2003).

[13] A. Muriel, in *Coherent Structures in Complex Systems*, edited by L. L. Reguerra, J. M. Bonilla, and J. M. Rubi, (Springer, Berlin, 2002).

[14] L. Jirkkovsky and L. Bo-ot, Physica A **352**, 241 (2005).

[15] S. A. Novopashin and A. Muriel, in *Engineering Turbulence Modeling and Experiments 5*, edited by W. Rodi and N. Fueyo (Elsevier, Amsterdam, 2002).

[16] S. A. Novopashin and A. Muriel, JETP Lett. **68:7**, 557 (1998).

[17] O. A. Nerushev and S. A. Novopashin, JETP Lett. **64:1**, 47 (1996).

[18] O. A. Nerushev and S. A. Novopashin, Phys. Lett. A **232**, 243 (1997).

[19] L. D. Hinkle and A. Muriel, J. Vac. Sci. Technol. A **23**, 676 (2005).

[20] S. A. Novopashin and A. Muriel, Source Tech. Phys. Lett. **26:3**, 231 (2000).

[21] S. Novopashin and A. Muriel, Phys. Lett. A **335**, 435 (2005).

[22] J. M. Florian, J. Plasma Phys. **482**, 17 (2003).

[23] K. C. Sahu and R. Govendarajan, J. Fluid Mech. (to be published).

[24] V. Stern and F. Hussain, J. Fluid Mech. **309**, 1 (1966).

[25] G. Broze and F. Hussain, J. Fluid Mech. **311**, 37 (1966).

[26] B. Yu. Zanin, J. Appl. Mech. Tech. Phys. **38**, 724 (1997).

[27] R. R. Mankbadi, *Transition, Turbulence and Noise: Theory and Applications for Scientists and Engineers* (Kluwer, Boston, MA, 1994).